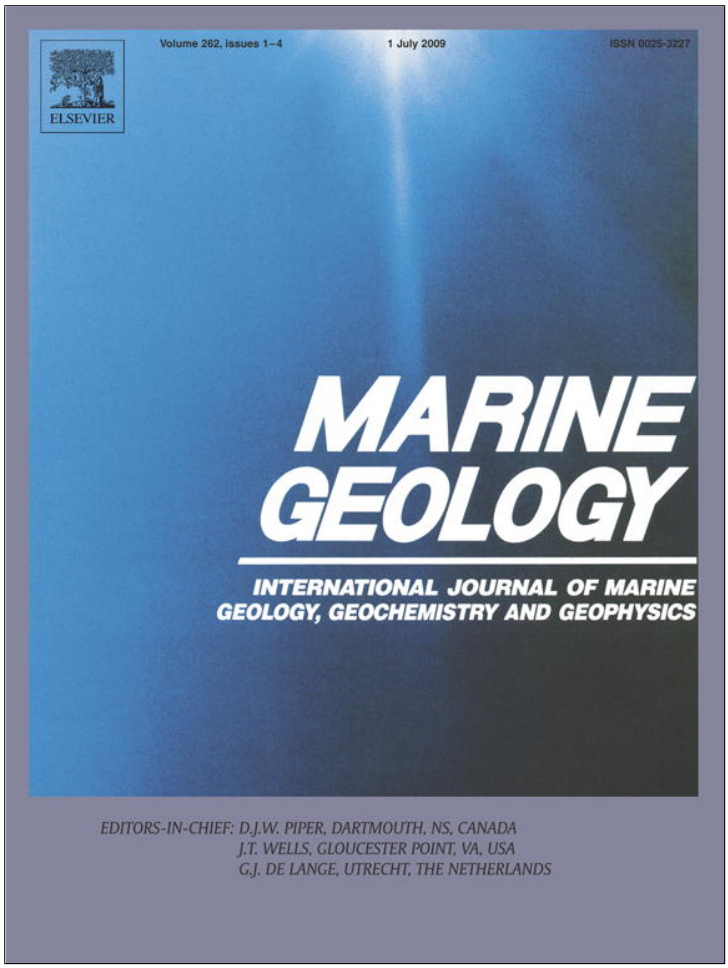

Marine Geology 262 (2009) 116–129

Contents lists available at ScienceDirect

Marine Geology

journal homepage: www.elsevier.com/locate/margeo

Seasonal variations in wave characteristics around a coral reef island, South Maalhosmadulu atoll, Maldives

P.S. Kench [a,*], R.W. Brander [b], K.E. Parnell [c], J.M. O'Callaghan [d]

[a] School of Geography and Environmental Science, University of Auckland, Private Bag 92019, Auckland, New Zealand
[b] School of Biological, Earth and Environmental Sciences, University of New South Wales, Sydney NSW 2052, Australia
[c] School of Earth and Environmental Sciences, James Cook University, Townsville, QLD 4811, Australia
[d] National Institute of Water and Atmosphere, Wellington, New Zealand

ARTICLE INFO

Article history:
Received 24 December 2008
Received in revised form 26 March 2009
Accepted 28 March 2009

Communicated by J.T. Wells

Keywords:
reef islands
hydrodynamics
coastal morphodynamics
Indian Ocean

ABSTRACT

Synchronous measurements of waves were made at six locations around a small reef platform island in the Maldives during both westerly and northeast monsoon conditions. Summary statistics of wave records indicated similar *Hs* values propagating onto windward and leeward reef surfaces and a distinct growth in wave height as waves shoal toward island shorelines. Waves up to 0.78 m were recorded impacting the island shoreline. Wave energy on the reef platform was strongly modulated by seasonal winds with wave energy during the westerly monsoon an order of magnitude larger than wave conditions in the northeast monsoon. Spectral analysis of wave records highlighted spatial differences in wave energy around the island. Windward reefs and shorelines are dominated by waves at wind and swell frequencies, whereas wind-wave energy is absent from leeward shorelines. Consequently, windward shorelines have up to twice the gross energy input than leeward shorelines. Results have significant implications for geomorphic processes. Longer duration and greater incident wave energy during the westerly monsoon has promoted higher growth of the western reef flat (+0.2 m) and more energetic shoreline runup processes have produced markedly higher western island ridges (+0.7 m). Incident shoreline wave processes are sufficient to entrain beach sediments during both monsoon periods although periods of active sediment mobilisation are constrained to mid- to high-tide stages. The windward–leeward gradient in shoreline wave energy is likely to drive littoral sediment flux. Seasonal modulation of the shoreline wave energy gradients account for observed oscillations in beach position around island shorelines. Large differences in incident wave energy between monsoons is considered to affect the rate of beach change around island shorelines rather than the total volumetric movement of island beaches.

1. Introduction

The interaction of incident ocean swell with coral reefs is widely known to modulate oceanographic, ecological and geological processes in coral reef systems (Hamner and Wolanski, 1988; Nakamori et al., 1992; Roberts et al., 1992; Abelson and Denny, 1997; Hearn et al., 2001). Incident waves and their interaction with coral reef platforms are also acknowledged as the main mechanism controlling the formation and stability of low-lying coral reef islands (Gourlay, 1988). The interaction of waves with reefs and their influence on the geomorphic development of islands is manifested in two ways. First, coral reef platforms act to filter incident ocean swell and control the energy that leaks on to reef platform surfaces. Second, the planform configuration of reefs both refracts and diffracts wave energy which controls the current patterns on reef surfaces and the development of nodal locations for island deposition.

The physical processes of wave breaking at the reef edge have been well documented. Numerous studies have documented large reductions in wave energy of up to 97% as incident swell is transformed and breaks at the reef edge (Roberts et al., 1977; Lee and Black, 1978; Gerritsen, 1981; Roberts and Suhayda, 1983; Young, 1989; Hardy et al., 1990; Lugo-Fernández et al., 1994; 1998; Hearn, 1999; Massel and Brinkman, 1999). However, there has been comparatively little emphasis placed on examining the character and importance of wave processes on reef flats for the formation, change and stability of reef sedimentary landforms such as beaches, sand aprons and reef islands.

Despite dramatic energy losses at the reef edge, residual wave energy still leaks onto reef flat surfaces. Transmission of this energy onto reef surfaces is greatest at higher water stages (Roberts et al., 1977; Brander et al., 2004) and in situations where the wave height is small compared with water depth resulting in wave propagation

* Corresponding author. Tel.: +64 9 373 7599x88440; fax: +64 9 373 7434.
E-mail addresses: p.kench@auckland.ac.nz (P.S. Kench), rbrander@unsw.edu.au (R.W. Brander), kevin.parnell@jcu.edu.au (K.E. Parnell), j.ocallaghan@niwa.co.nz (J.M. O'Callaghan).

0025-3227/$ – see front matter © 2009 Elsevier B.V. All rights reserved.
doi:10.1016/j.margeo.2009.03.018

across the reef crest with minimal breaking (Kench and Brander, 2006a). Although the formation and character of reformed waves on reefs have been described (Hardy et al., 1990; Nelson, 1994; Lugo-Fernández et al., 1994; Gourlay, 1994, 1996; Massel, 1996; Nelson, 1997), the subsequent propagation and transformation of such wave energy across reef flats toward island shorelines has received much less attention. Understanding such processes is fundamental to resolving controls on geomorphic development and change of island shorelines.

In recent studies, Brander et al. (2004) examined across reef variations in wave energy at Warraber Island, Torres Strait and identified the importance of relative water depth across reefs in controlling the delivery of wave energy to island shorelines. Kench and Brander (2006a) and Samosorn and Woodroffe (2008) also highlighted the fact that the energetics of leeward island shorelines may be greater than windward shorelines due to the differential wave dissipation role of reef flats, which in turn is dependent on reef width and elevation (Lowe et al., 2005). These studies highlight the fact that wave processes are not uniform around reef island shorelines.

Recognition of such spatial differences in wave generated processes highlights the susceptibility of reef island geomorphology to changing process regimes, as incident ocean wave climates vary in magnitude and direction at event, seasonal and decadal timescales. As wave direction changes, islands may be subject to altered nearshore wave conditions which are likely to affect sediment entrainment and transport processes on reef surfaces and island shorelines. However, few studies have attempted to examine wave behaviour around the shoreline of reef islands or investigate how climate driven variations in incident wave energy may alter nearshore wave processes.

This study examines the characteristics and transformation of waves and wave energy propagating onto a circular reef platform that supports a reef island. Experiments are based on synchronous measurements of waves at six locations on a reef platform around a reef island. Specific objectives of the study are to: i) identify the spatial and temporal variations in wave characteristics propagating onto reef flat surfaces; ii) determine the transformation of waves to island shorelines; iii) examine spatial differences in wave energy around island shorelines; and iv) determine the effect of predictable changes in monsoon seasons on the magnitude and character of reef flat wave processes.

2. Field setting

Measurements were conducted on a circular reef platform in South Maalhosmadulu atoll, located in the Maldives archipelago, central Indian Ocean (Fig. 1). The Maldives comprise 21 atolls and 4 oceanic reef platforms that extend over 860 km from 6°57′ N to 0°34′ S. The archipelago consists of a double chain of atolls either side of an inner sea, tapering to single atolls to the north and south (Fig. 1b). Situated in the central and western side of the archipelago, South Maalhosmadulu atoll is approximately 40 km in width and length (Fig. 1c). The atoll has a total surface area of 1127 km^2, with 105 reefs (peripheral

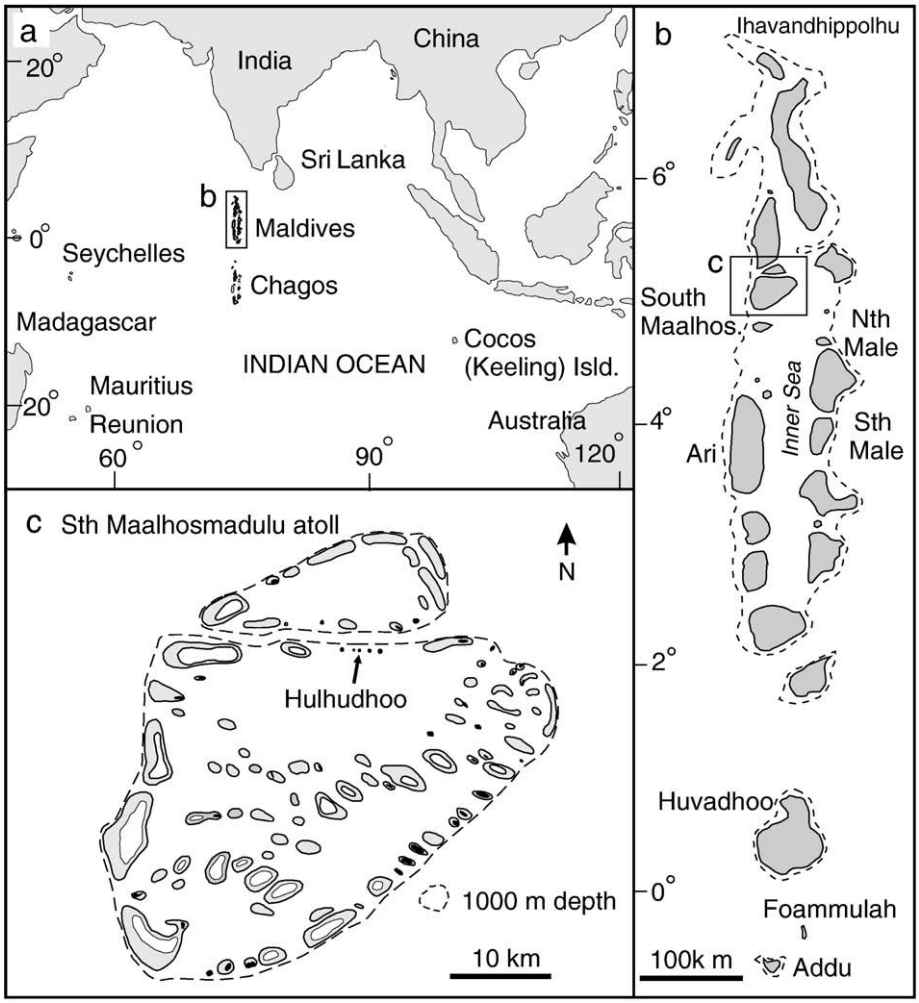

Fig. 1. Location of Hulhudhoo reef platform, South Maalhosmadulu atoll, Maldives: a) location of Maldives archipelago; b) Configuration of the Maldives archipelago; c) Planform configuration of South Maalhosmadulu atoll showing location of Hulhudhoo Island.

and lagoonal totalling 262.9 km^2) and 56 reef islands totalling 5.50 km^2 (2.1% of total reef area, Naseer and Hatcher, 2004). The atoll rim is discontinuous characterised by numerous passages up to 40 m deep and 4500 m wide. Consequently, the effective aperture of the atoll rim is 37% allowing oceanic currents and waves to penetrate the lagoon.

2.1. Hulhudhoo reef platform

The focus of this study is the Hulhudhoo reef platform in the central and northern part of the atoll lagoon (Figs. 1c and 2). This reef platform was chosen due to its circular shape, which is approximately 400 m in diameter (Fig. 2) and has a surface area of approximately 85,512 m^2. The reef is considered an ideal field laboratory to examine the effect of changing wave processes on the simplest (circular) reef structure. The platform rises steeply from lagoon water depths of 60–80 m where there is a marked transition at the reef edge to a near horizontal reef flat surface.

The outer reef edge lacks the typical buttress or algal rim morphology found in exposed reef systems and exhibits a gradual decline in elevation from the central reef flat to a sharp seaward drop off (Fig. 2). Measured reef edge elevation varies from 1.04 m below msl (bmsl) on the southwest to 1.58 m bmsl on the northeastern side of the platform (Table 1). The outer reef flat surfaces are generally characterised by a living outer reef flat containing live *Porites*, *Acroporid* and *Millepora* sp. There is an ecological and morphological transition from the living reef flat surface to a lower elevation surface composed of coral rubble and sand within 20–50 m of island shorelines referred to as the 'moat' (Fig. 2). This transition is commonly characterised by a vertical step (0.3 to 0.8 m in elevation) to the lower 'moat' surface which ranges in elevation from 0.77 to 0.86 m bmsl on the southern sectors of the reef to 1.43 m bmsl in the northeast (Fig. 2; Table 1). The moat encircles the island (Fig. 2).

Table 1
Summary of physical characteristics of Hulhudhoo reef platform.

	Reef edge elevation (m)	Max. Elevation of coral on outer reef (m)	Mean outer reef flat elevation (m)	Moat elevation (m)	Island ridge elevation (m)	Reef width (m)
Southwest	−1.04	−0.66	−0.73	−0.86	2.51	48
Northwest	−1.55	−0.64	−0.93	−1.16	1.92	35
Northeast	−1.58	−0.63	−1.20	−1.43	1.36	42
Southeast	−1.71	−0.47	−0.80	−0.77	1.63	34

Location of reef and physical properties shown in Figs. 1 and 2. All elevations are relative to mean sea level.

The reef platform contains a small sand cay of mid-Holocene age (Kench et al., 2005) that mirrors the shape of its reef platform (Fig. 2). Hulhudhoo Island occupies 49% of the reef area and is situated in the centre of the reef platform surface. Reef width (distance from reef edge to toe of beach) is narrow around the island ranging from 34 m in southeast to 48 m on the southwest (Fig. 2; Table 1). The cay has maximum island ridge elevations that range from 2.51 m above msl on the southwest to 1.36 m above msl on the northeast shoreline. A mobile sand beach surrounds the shoreline and has been found to exhibit significant morphological variation between seasons (Kench and Brander, 2006b).

2.2. Climate and oceanographic regime

The Asian monsoon is a pervading influence on the climate of the Maldives with two main monsoon periods marked by strong

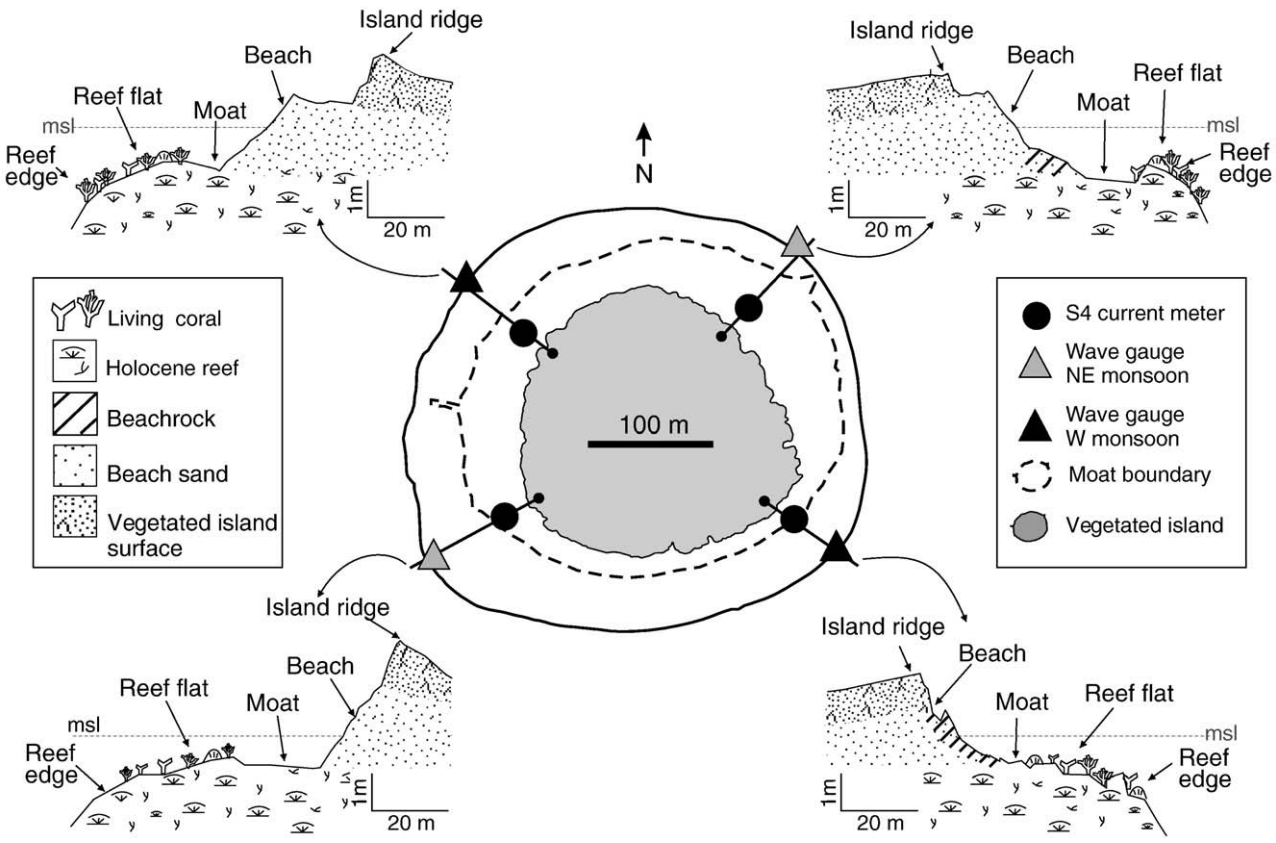

Fig. 2. Hulhudhoo reef platform showing location of wave gauges and island to reef topographic profiles. Note variation in reef elevation between profiles.

reversals in wind direction (Fig. 3a, b). Between April and November the archipelago is subject to the westerly monsoon with winds from the southwest–northwest (~225–315°) with a mean wind speed of 5.0 m s^{-1}. From November to March the northeast monsoon generates winds from the east–northeast (~45–90°) with a mean wind speed of 4.8 m s^{-1} (Fig. 3a, b, Department of Meteorology, 1995). Wind data recorded during the field experiments show that both the direction and speed of wind was consistent with the long-term climate records, with west–northwest winds prevalent during the June 2002 experiment and northeast winds occurring during the February 2003 deployment (Fig. 3c, d).

The archipelago is subject to a semidiurnal microtidal regime with spring and neap tidal ranges of 1.2 m and 0.6 m respectively. Information on the deepwater wave climate is limited, but satellite altimetry derived wave climate data over a ten-year period for the region (Young, 1999) indicates the dominant swell approaches from southerly directions (Fig. 4). On a seasonal basis, swell is from the south-southwest from April to November with a peak significant wave height (*Hs*) of 1.8 m in June, and from the south to southeast directions from November to March with minimum *Hs* of 0.75 m in March (Fig. 4).

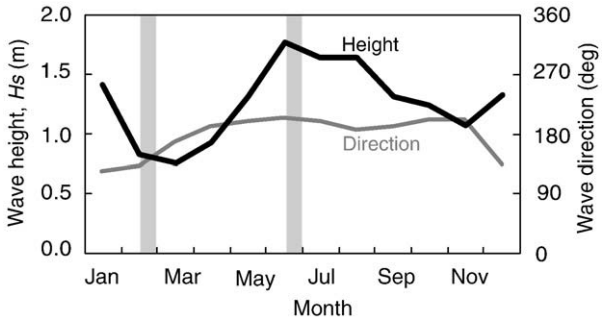

Fig. 4. Ten year mean monthly ocean swell height (black line) and swell direction (grey line) for the central Maldives. Data from Young (1999). Grey vertical bars identify periods of measurement on Hulhudhoo.

3. Methods

Experiments were undertaken on Hulhudhoo reef platform in June 2002 and February 2003, corresponding to maxima and minima incident ocean swell conditions (Fig. 4) during westerly and northeast monsoon conditions respectively (Fig. 3). Four days of measurements were undertaken in each season to document the characteristics of waves propagating onto the reef platforms, the transfer of energy to island shorelines, and the variability in wave properties around the island shorelines. Dobie wave gauges were deployed at the reef edge to record outer reef flat wave conditions on both the windward and leeward exposures of the reef platform. Consequently, the location of these outer instruments was altered between experiments (Fig. 2). The Dobies sampled at 2 Hz for 17.07 min (2048 samples) every 30 min. Water depths (h) at these reef flat locations were less than 2.5 m throughout the experiments.

Four InterOcean S4 electromagnetic current meters and wave recorders were deployed in positions around the island, within 10 m of the island shoreline (in the moat) to record wave energy propagating to the island beaches (Fig. 2). The locations were selected to synchronously document wave properties on different exposures of the island. While located in the nearshore, sites were selected to characterise shoreline wave energy and are hereafter referred to as shoreline locations. The S4s were mounted on stainless steel pods 0.2 m from the bed. Due to varying memory capacity of the S4 current meters differing setup routines were adopted. However, all instruments sampled at a minimum frequency of 2 Hz for 20 min each hour. Water depths (h) were less than 1.5 m during experiments and signal attenuation with depth was negligible.

Estimates of significant wave height (*Hs*), maximum wave height (*Hmax*), significant wave period (*Ts*) and mean wave period (*Tz*) were determined by zero-downcrossing analysis. Spectral analysis was

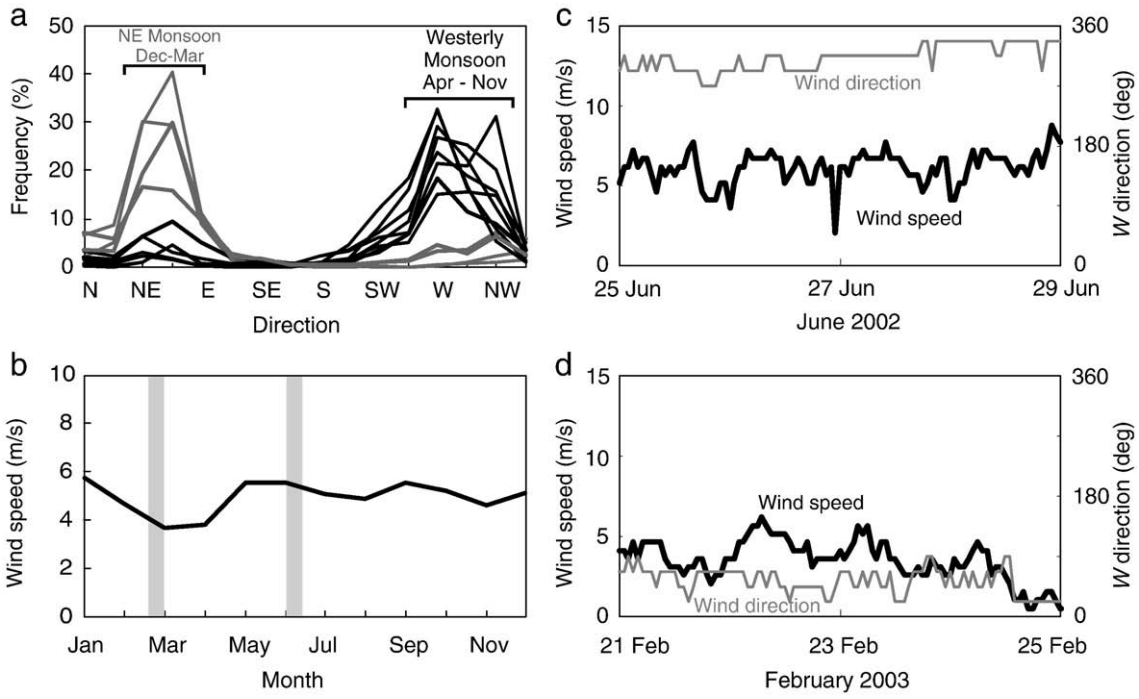

Fig. 3. Summary wind data for the Maldives archipelago: a) 30-year mean monthly percent frequency wind direction; b) 30-year mean monthly wind speed. Climate data from Government of Maldives, Department of Meteorology, 1995; c) measured wind speed and wind direction during the June 2002 wave experiment; d) measured wind speed and direction during the February 2003 wave experiment. Grey vertical bars identify periods of measurement on the Hulhudhoo reef platform.

performed using Welch's averaged modified periodogram method of spectral estimation (Welch, 1967) to determine the variance associated with energy at specified wave frequencies. Analysis was performed on the first 17.07 min (2048 samples) of every hour for the S4 data and for every 30 min period for the Dobie data. All data were analysed with 8 degrees of freedom. Wave energy was partitioned into four frequency bands reflecting differences in the wave generation mechanism: very short period waves with frequencies of 0–0.333 Hz (0–3 s); wind-waves with frequencies of 0.333–0.125 Hz (3–8 s); swell-waves with frequencies of 0.125–0.05 Hz (8–20 s); and infragravity waves with frequencies of <0.05 Hz (>20 s). The proportion (%) of energy within each frequency band in a given time series record was computed by dividing the variance in that band by the total variance in the time series.

4. Results

4.1. Westerly monsoon wind and wave summary

Winds during the June deployment blew consistently from the northwest and ranged in speed from 4 to 8 m s^{-1} (Fig. 3c). Tides on the reef platform were semidiurnal with a strong diurnal inequality and tidal excursions ranged from 0.20 m to 1.0 m. (Fig. 5a). Higher water levels on the reef platform were sustained during low amplitude tidal excursions.

Summary wave statistics for the westerly monsoon deployment are presented in Fig. 5a–f and Table 2. Mean *H*s values at the outer reef flat ranged from 0.19 m to 0.23 m with *T*s values of 6.2 and 10.1 s, for the windward (NW) and leeward (SE) locations. Notably, the outer reef time series do not exhibit evidence of tidal modulation suggesting that recorded waves represented incident wave conditions at the reef edge (Fig. 5a, f). Maximum recorded wave heights at the outer reef flat were 0.43 m and 0.59 m for the windward and leeward locations respectively. There is also a small reduction in wave *H*s values through the measurement period.

Mean *H*s values from the nearshore instruments ranged from 0.16 m (SW) to 0.25 m (SE) with corresponding *T*s values of 6.2 and 9.0 s (Fig. 5; Table 2). Unlike the outer reef flat, shoreline waves were tidally modulated with peak *H*s values corresponding to high tide stages ranging from 0.26 m on the northeast to 0.41 m on the southeast locations (Fig. 5; Table 2). Maximum shoreline wave heights were 0.66 m and 0.78 m on the windward western locations and are lower (0.46–0.59 m) on the leeward eastern side of the island. Wave heights were generally higher at the southeastern shoreline (Table 2). Of note, waves at the northeast shoreline do not exhibit strong tidal modulation and consistently have lower heights than other locations (Fig. 5d).

4.2. Northeast monsoon wind and wave summary

The February 2003 measurement period was characterised by winds from the east–northeast ranging in speed from 2 to 6 m s^{-1} (Fig. 3d). Semi-diurnal tides on the reef platform exhibited a marked diurnal inequality with largest tidal excursions up to 0.8 m (Fig. 5g). Smaller tidal excursions were approximately 0.2–0.3 m indicating that higher water levels on the reef platform were sustained during these low amplitude tidal excursions. Summary wave characteristics on the reef platform show that incident wave conditions were significantly lower in magnitude during the northeast monsoon with mean *H*s values all below 0.10 m (Fig. 5g–l).

Outer reef flat wave heights were not significantly tidally modulated and were similar in magnitude with mean and maximum *H*s values of 0.07 m and 0.11 m on the outer windward reef and 0.06 and 0.12 m on the leeward reef (Fig. 5g, l; Table 2). *T*s and *H*max were 5.8 s and 0.19 m on the windward reef flat and 7.6 s and 0.26 m on the leeward reef flat respectively.

Shoreline waves were also characterised by small wave heights with mean *H*s ranging from 0.06 m to 0.09 m. Similar to conditions during the westerly monsoon, tidal modulation was apparent in all but the northeast shoreline records. Peak *H*s values ranged from 0.09 m on the northwest to 0.14 m at both easterly exposed shorelines (Table 2). *T*s values ranged between 4.9 and 6.6 s. Maximum shoreline wave heights were 0.21 and 0.24 m on the northeast and southeast respectively (Fig. 5h–k).

4.3. Spatial variations in wave energy spectra: westerly monsoon

Wave energy spectra were computed for all 1294 data bursts from both experiments. Examination of spectra indicated consistent changes in energy occurring on the reef and nearshore associated with critical water elevations. Wave spectra across one rising tide are summarised in Table 3 and a selection of spectra from this rising tide period are presented in Fig. 6. Rising tide spectra on June 26th are presented for low water, mid-tide and high tide stages (Fig. 6a–f). As noted previously the atoll experiences a microtidal regime with the tidal range on the Hulhudhoo reef being 1.0 m on June 26th. Consequently, the mid-tide times selected reflect approximately 0.6 and 0.4 m water level increments.

Results highlight a number of key features of wave characteristics on the reef platform. First, waves on the reef platform are generally contained in the swell wave band with frequencies ranging from 0.09 to 0.13 Hz (Table 3). Exceptions are the southeast shoreline at low tide and the southwest shoreline at low to mid-tidal stages where peak energy is contained at infragravity frequencies (Table 3). Second, there is little change in the peak frequency of waves on the reef platform at different tidal stages (Table 3).

Third, the outer reef flat experiences relatively consistent total wave energy inputs at different tidal stages (Table 3, Fig. 6a, f). Indeed, higher energy values at low tide are likely to reflect wave shoaling at the outer reef. Fourth, and in contrast to outer reef sites, shoreline waves show a significant increase in total spectral energy as tidal stage increases (Table 3; Fig. 6). At low tide shoreline wave energy is small (as reflected in individual spectra, Fig. 6b–e) as the low water depth filters waves from traversing the reef surface. However, there is a marked increase in total spectral energy at mid- and high-tide as the water depth constraint is exceeded allowing wave energy to propagate to the shoreline.

Fifth, there are spatial differences in total wave energy inputs. As noted above, the total energy remains relatively constant at outer reef flat locations. At nearshore locations there are distinct differences in spectra between the windward (westerly) and leeward (easterly) sites (Fig. 6b–e). While all exhibit a dominant energy peak at swell frequencies between 10 and 10.6 s (0.09–0.1 Hz), spectral densities (energy) are significantly greater in magnitude at westerly sites. Indeed, windward shoreline locations (NW and SW) have more than twice the total wave energy than leeward shoreline locations at highest tide (Table 3).

The fact that peak wave frequency is stable at most sites throughout the rising tide masks differences in the character of wave spectra between instrument locations (Fig. 6a–f), which account for the differences in total energy at the shorelines. In particular, all westerly reef and shoreline locations also contain energy at wind wave frequencies with minor peaks in energy ranging between 0.16 Hz and 0.19 Hz (5.2–6 s). Both the windward shoreline locations also exhibit minor peaks in energy at infragravity frequencies. In contrast, easterly shorelines exhibit narrow peaks in energy at swell frequencies, but energy at wind wave frequencies is comparatively absent (Fig. 6d, e).

4.4. Spatial variations in wave energy spectra: northeast monsoon

A summary of wave spectra across a rising tide (0.8 m tidal range) on February 22nd shows both similarities and differences in the character and energy of waves on the Hulhudhoo reef platform under

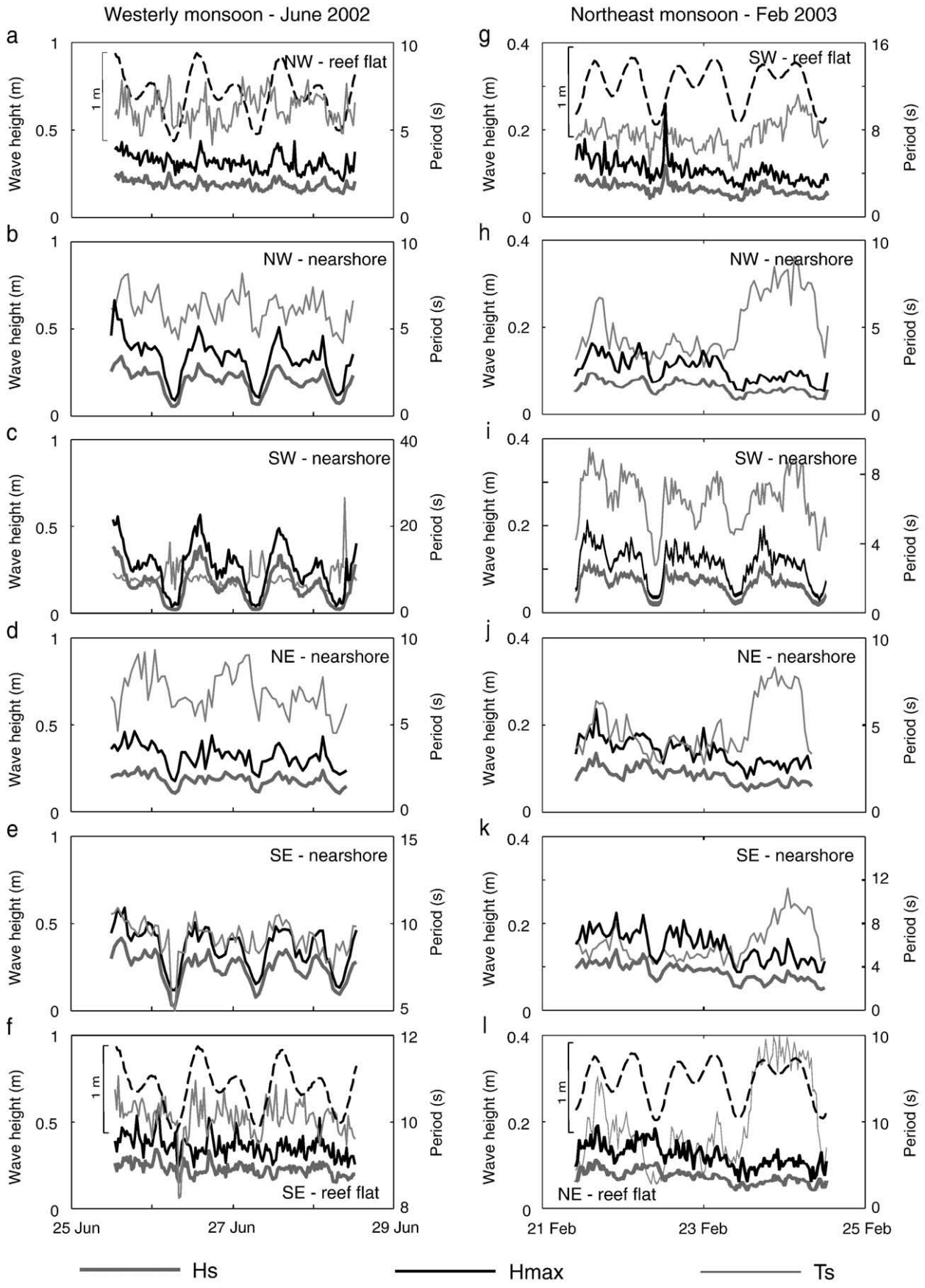

Fig. 5. Summary wave statistics for each instrument location on Hulhudhoo reef platform. a–f) June wave measurements; g–l) February wave measurements. Location of instruments identified in each figure and shown on Fig. 2. Dashed lines in a and g represent water level.

Table 2
Summary of wave characteristics during wave experiments on Hulhudhoo.

Location		*Hs*		*Hmax*		*Ts* (s)	*Tz* (s)
		Mean (m)	Peak (m)	Mean (m)	Peak (m)		
West monsoon							
Windward RF	NW	0.19	0.25	0.31	0.43	6.2	4.3
Leeward RF	SE	0.23	0.34	0.36	0.59	10.1	8.2
Shoreline	SW	0.16	0.38	0.27	0.78	8.0	4.6
	NW	0.20	0.34	0.33	0.66	6.2	4.0
	NE	0.18	0.26	0.32	0.46	6.8	4.2
	SE	0.25	0.41	0.36	0.59	9.2	5.9
Northeast monsoon							
Windward RF	NE	0.07	0.11	0.12	0.19	5.8	4.3
Leeward RF	SW	0.06	0.12	0.10	0.26	7.6	5.3
Shoreline	SW	0.07	0.12	0.12	0.21	6.6	4.3
	NW	0.06	0.09	0.10	0.16	5.1	3.7
	NE	0.08	0.14	0.14	0.24	4.9	3.4
	SE	0.09	0.14	0.15	0.22	6.1	4.2

RF = reef flat.

northeast monsoon conditions (Table 3; Fig. 6g–l). First, spectral energies (individual and total) are an order of magnitude less than during the westerly monsoon, which is a direct indication of reduced wave energy conditions experienced under northeast monsoon conditions. Second, like the westerly monsoon peak wave frequencies are in the swell energy band (Table 3). Notable exceptions are the prevalence of infragravity energy at the southwest shoreline at low tide and higher frequency energy at the windward (northeast) outer reef and shoreline at low tide.

Third, despite the dominance of swell energy, spectra from all sites are characterised by a spread of energy across both swell and wind-wave frequencies. At shoreline locations, low tide spectra are dominated by energy at swell frequencies (e.g. 0.107 Hz, 9.3 s in the southeast), but as water depth increases the spectra develop multiple peaks. Peak energy still occurs in the swell energy band, but shifts to lower frequencies (e.g. 0.08 Hz, ~12.5 s) in the southeast and southwest (Fig. 6i, k). Secondary peaks are present at wind wave frequencies generally clustering around 0.15–1.8 Hz (~6.6–5.6 s) with broader peaks around 0.25 Hz (4 s; Fig. 6h, i, k). Energy at infragravity frequencies is only present at high tide at the southwest shoreline (0.015 Hz, ~67 s; Fig. 6i). Fourth, there is a general, yet small, increase in total spectral energy with tidal stage at shoreline locations, with the most abrupt change at mid-tide (Table 3). Finally, the windward southeast shoreline possesses the largest spectral energies of all sites at mid- to high-tide stages.

5. Discussion

Wave measurements on the Hulhudhoo reef platform show that waves of similar magnitudes, but having a range of frequencies are able to propagate onto the reef surface and reach island shorelines during each monsoon season. During the stronger westerly monsoon, shoreline *Hs* and *Hmax* peaked at 0.26–0.41 m and 0.46–0.78 m respectively (Table 2) indicating that sufficient energy impacts shorelines to stimulate geomorphic work. However, results of this study also highlight marked spatial and seasonal differences in wave characteristics across the reef platform and around the island shoreline. Physical reasons for these observations and their geomorphic implications are now discussed.

5.1. Cross reef variations in wave height

Summary statistics of wave measurements from the Hulhudhoo reef platform during the westerly monsoon conditions indicate that wave heights (*Hs*) were broadly similar at outer reef flat and shoreline locations. Maximum differences in mean and peak *Hs* values between sites are 0.09 m and 0.16 m respectively (Table 2). Perhaps counter intuitively however, wave measurements show that the leeward southeast outer reef flat had consistently higher waves than the windward northwest reef flat.

During northeast monsoon conditions, wave energy (*Hs*) was considerably lower and *Hs* and *Hmax* showed only minor variations of 0.02 m and 0.05 m respectively between all sites (Table 2). However, despite the low wave energy conditions, both the windward northeast and southeast nearshore locations consistently experienced marginally greater wave height than the leeward western side of the island.

Results also show that measured wave heights were consistently larger at shorelines compared with outer reef sites. Fig. 7 provides a comparison between outer reef flat and adjacent shoreline wave heights for windward and leeward exposures for both monsoonal measurement periods. During the westerly monsoon *Hs* was higher at the northwestern shoreline than the outer reef flat for 73% of the monitoring period (Fig. 7a). Shoreline *Hs* values were up to 45% larger than reef flat waves (mean increase of 21%) while *Hmax* values showed increases of up to 72%. Of note, the largest amplification of shoreline waves corresponded with higher tidal stages. Similar results were found at the southeastern shoreline where shoreline wave heights were larger than reef edge waves for 61% of the measurement period with mean amplification of *Hs* by 23% ranging to a maximum of 68% (Fig. 7b). At both sites, periods in which wave height actually decreased from the outer reef to the nearshore (28% and 38% for the northwest and southeast locations respectively) corresponded only with lower water stages (Fig. 7b).

Table 3
Summary of wave spectral characteristics during wave experiments on Hulhudhoo.

Location		Spectral peak (Hz)					Total energy variance (m^2/Hz)				
		LW	+2	+4	+6	HW	LW	+2	+4	+6	HW
West monsoon — 26 June 2002											
Windward RF	NW	0.10 [19]	0.10 [25]	0.10 [59]	0.12 [18]	0.1 [29]	3.3	2.3	3.4	2.1	4.8
Leeward RF	SE	0.10 [41]	0.10 [38]	0.10 [44]	0.11 [41]	0.11 [65]	4.5	2.0	4.2	2.3	2.8
Shoreline	SW	0.01 [95]	0.01 [86]	0.01 [12.6]	0.10 [47]	0.10 [42]	0.1	0.1	3.3	5.4	10.2
	NW	0.13 [12]	0.10 [13]	0.10 [69]	0.11 [52]	0.10 [50]	0.3	0.6	4.1	3.8	7.6
	NE	0.09 [37]	0.09 [40]	0.10 [64]	0.10 [45]	0.10 [38]	1.1	1.4	3.9	2.9	3.3
	SE	0.01 [33]	0.10 [39]	0.09 [61]	0.10 [32]	0.09 [37]	0.1	0.8	4.8	4.0	3.7
Northeast monsoon — 22 February 2003											
Windward RF	NE	0.34 [18]	0.07 [1.0]	0.08 [4]	0.08 [5.5]	0.08 [12.6]	0.9	0.4	0.6	0.5	0.6
Leeward RF	SW	0.10 [19]	0.11 [72]	0.11 [18]	0.12 [38]	0.11 [17]	0.3	0.5	0.4	0.5	0.4
Shoreline	SW	0.01 [4]	0.11 [84]	0.11 [25]	0.11 [13]	0.08 [12]	0.02	0.2	0.4	0.4	0.6
	NW	0.13 [4]	0.11 [13]	0.11 [18]	0.11 [8]	0.11 [19]	0.2	0.3	0.4	0.5	0.6
	NE	0.36 [0.9]	0.07 [0.7]	0.19 [3]	0.13 [11]	0.16 [4]	0.6	0.4	0.6	0.5	0.6
	SE	0.12 [9]	0.11 [50]	0.08 [69]	0.08 [10]	0.08 [8]	0.4	0.7	1.0	1.1	1.0

NB: Values in square bracket reflects peakedness of the spectrum values, low values reflect a broad flat spectrum, high values a peaked spectrum.

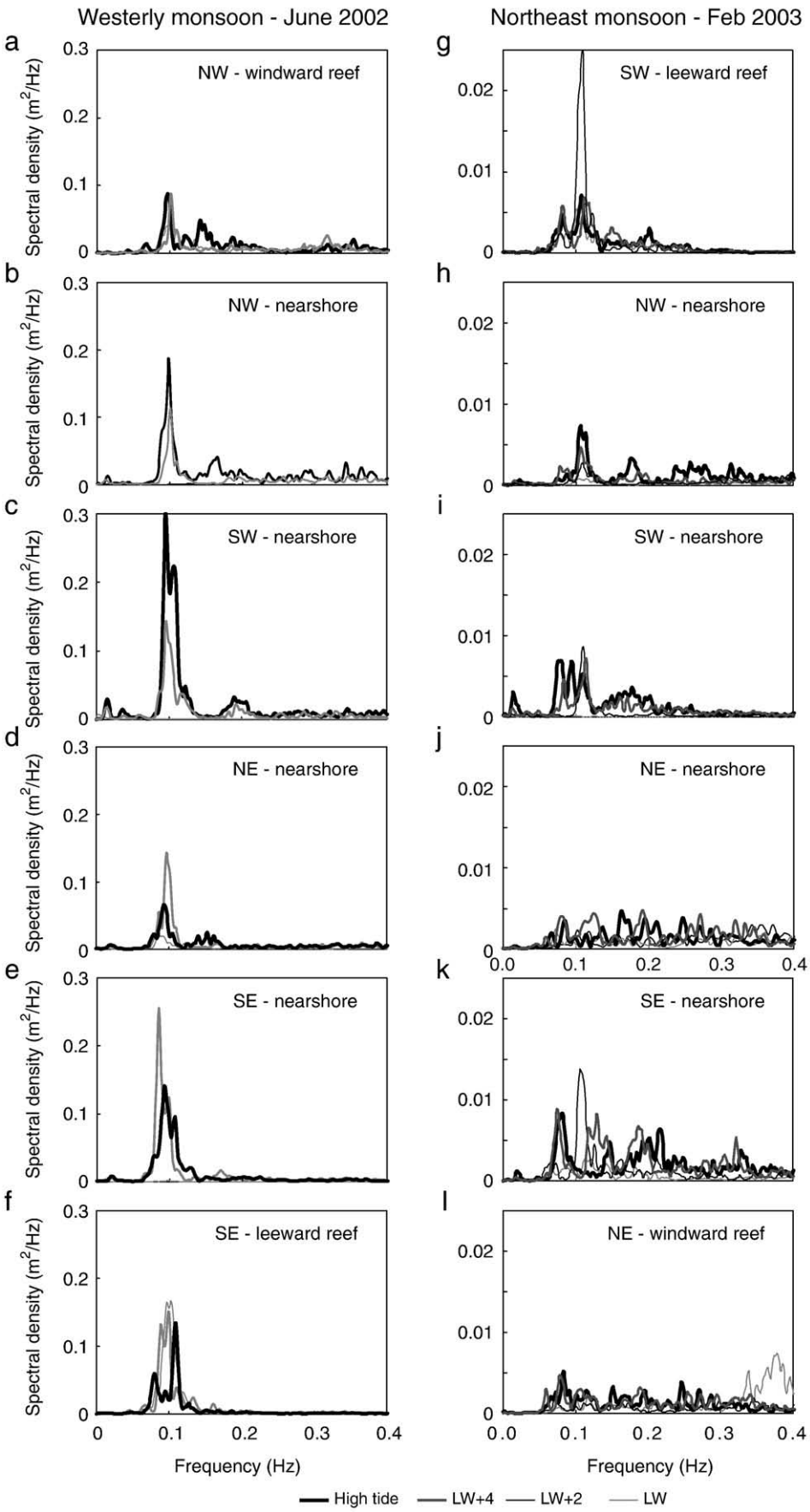

Fig. 6. Selected wave energy spectra at different tidal stages at each reef platform location on Hulhudhoo Island. a–f) June 26th 2002; g–l) February 22nd 2003. Spectra selected are for low, mid and high water levels. Note that the spectral density scale differs between the June and February data. Location of instruments identified in each figure and shown on Fig. 2.

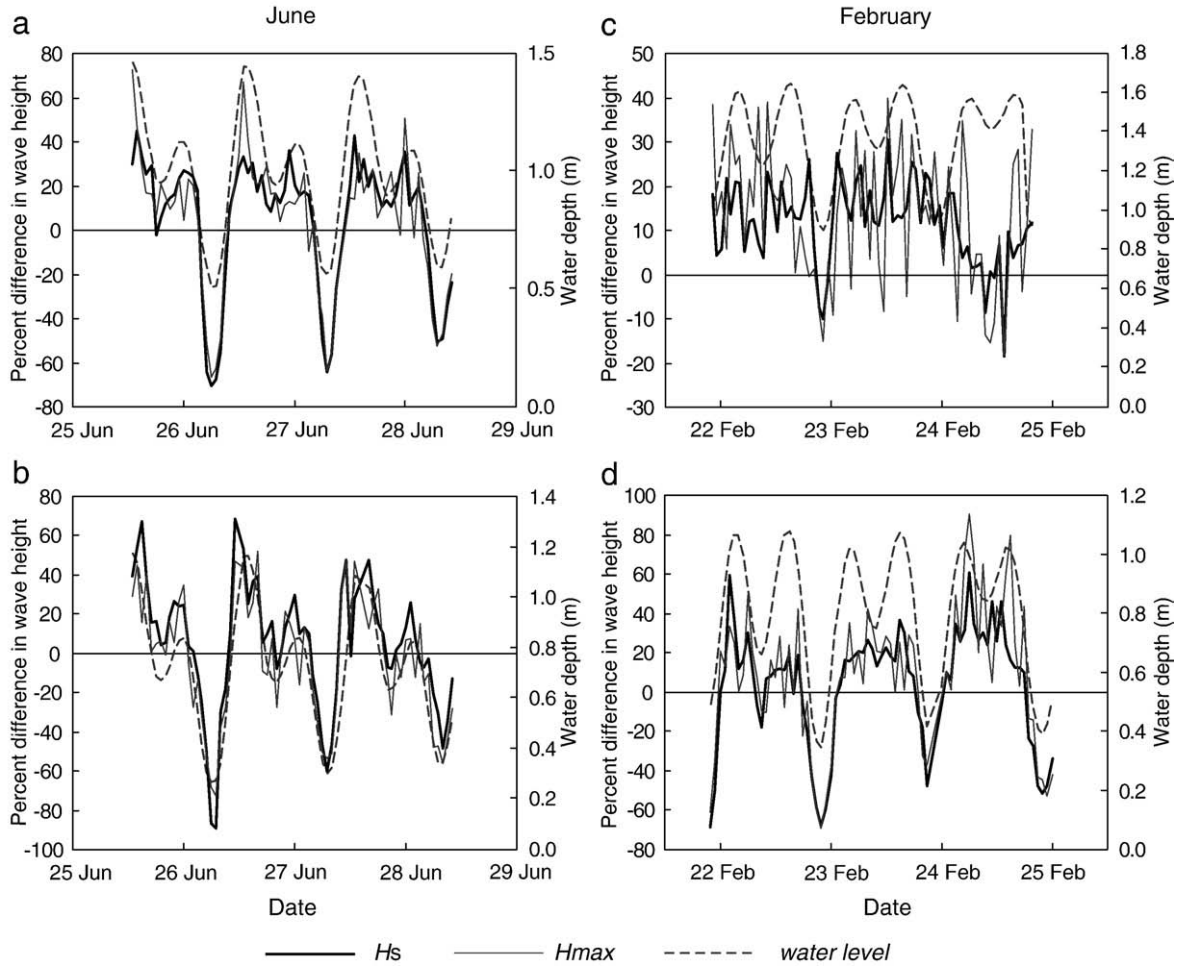

Fig. 7. Percentage change in wave height from outer reef flat to nearshore locations on a) the northwest (windward); and b) southeast (leeward) sides of Hulhudhoo during the westerly monsoon (June); c) northeast (windward); and d) southwest (leeward) sides of Hulhudhoo during the northeast monsoon (February). Positive values indicate a growth in wave height and negative values represent reduction in wave height at the island shoreline.

Similar transformations in wave height also occurred during northeast monsoon conditions. On the windward northeast aspect of the island, *Hs* values increased between the outer reef and shoreline for 92% of the measurement period (Fig. 7c) with mean and maximum increases in *Hs* of 14% and 38% respectively. In contrast to the westerly monsoon however, these changes did not exhibit a marked association with tidal stage (Fig. 7c). On the leeward southwest exposure of the island, shoreline increases in *Hs* occurred for 73% of the experimental period with mean and maximum transformations in *Hs* of 21% and 61% respectively (Fig. 7d).

These observations are unique as they identify a distinct growth in wave height and therefore wave energy density between the outer reef and nearshore locations. The reef surrounding Hulhudhoo is relatively narrow, extending only 34–48 m from the shoreline and observed increases in wave height in the nearshore must be attributed to wave shoaling from the outer reef locations across the shallow reef flats (Table 1). Increases in wave height at the island shoreline are positively correlated with increases in *Hs* values on the outer reef flat and indicate a growth in wave energy at swell frequencies toward the shoreline. These observations differ significantly from previous studies that have mainly documented cross-reef reductions in wave height (e.g. Roberts and Suhayda, 1983; Hardy et al., 1990; Roberts et al., 1992).

5.2. Spatial variation in wave height around the island shoreline

A direct comparison of shoreline wave heights on different exposures of the island (Fig. 8) highlights a number of spatial patterns in wave properties around the island. First, under higher wave energy westerly monsoon conditions, *Hs* is strongly modulated by water depth at most locations ranging from 0.05 m at low water to more than 0.35 m at high water (Fig. 8a). One exception was the northeast shoreline where *Hs* values ranged between 0.1 m and 0.25 m. Second, waves at the southeast and southwest shoreline were consistently larger (by 0.05 m) than the northwest shoreline at higher tidal levels (Fig. 8a). Third, during the lower wave energy northeast monsoon it is apparent that eastern shorelines consistently received higher waves (*Hs* ~0.05 m larger) than western shorelines (Fig. 8b).

These spatial and temporal differences in shoreline wave characteristics have a number of implications for activation of sediment transport at island shorelines. Strong modulation of shoreline wave height indicates that activation of the shoreline sediment transport system occurs in a temporal window constrained by mid- to upper tidal stages. Despite significant differences in wave conditions between seasons, wave heights of ~0.1 m are still sufficient to activate sediment flux at the shoreline. Consequently, gross energy differences are indicative of gross levels of geomorphic stimulation of the beach system. Data suggest that swell energy is not evenly distributed around the shoreline with a bias toward energy impacting southwest and southeastern shorelines.

5.3. Spatial variation in dominant wave frequencies and incident shoreline energy

Results show that spatial variations in the relative importance of wind and swell energy exist on the reef platform around Hulhudhoo (Fig. 6). These differences are summarised for the duration of both

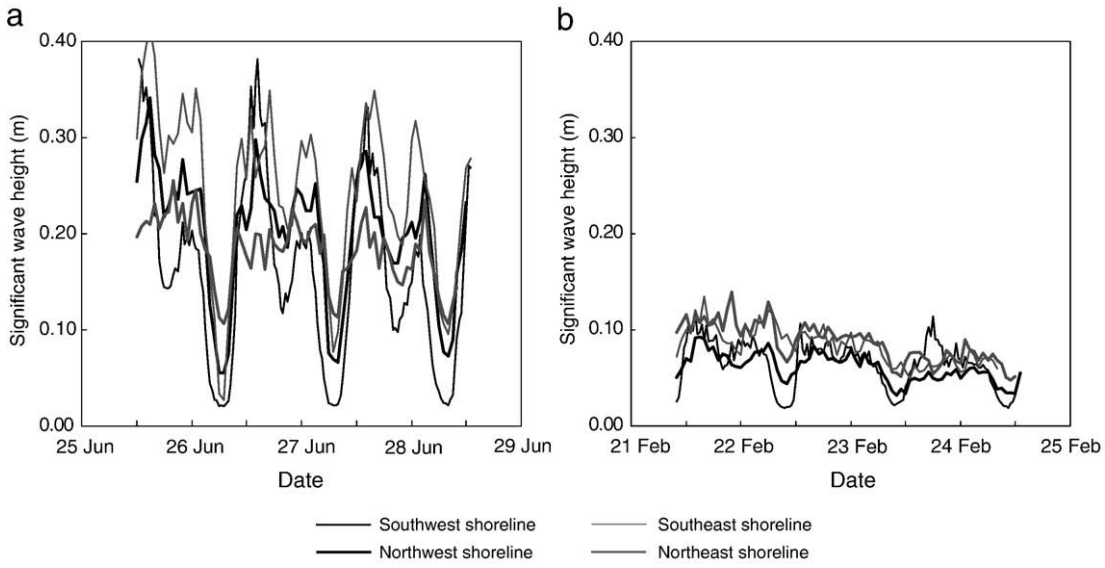

Fig. 8. Comparison of significant wave height values at nearshore instrument locations on Hulhudhoo Island. a) westerly monsoon (June); b) northeast monsoon (February).

measurement periods in Fig. 9. During the stronger westerly monsoonal wind conditions, energy at swell wave frequencies is dominant at most locations. However, the relative importance of swell wave energy changes from peak values of 40–50% at the windward outer reef and nearshore locations (northwest and southwest) to values of 60–75% on the leeward (eastern) shoreline and reef edge (Fig. 9a–f). The dominance of swell energy at all locations is considered to reflect the refraction of incident swell around the circular reef platform and its subsequent propagation to island shorelines.

The relatively lower importance of swell energy at windward locations is explained by the greater occurrence of energy at higher frequencies (wind wave and above, Fig. 9a–c). Wind-wave energy peaks at 20–40% at these locations as westerly driven wind-waves are able to propagate onto the windward reef and impact the western shoreline. In contrast, the importance of wind-wave energy reduces significantly at leeward locations and is generally less than 10–15% (Fig. 9e, f). This reduction is attributed to the orientation of the shorelines and protection from the prevailing wind direction. Wind-generated waves are less likely to refract across the relatively deep reef surface but continue to propagate eastward, oblique to the reef.

Energy at infragravity frequencies is minimal in all but the northwest outer reef flat and shoreline, where it increases at lower water levels (Fig. 9a, b). The general absence of infragravity energy is likely a consequence of the narrow reef flats which limit the potential for transformation of long waves on the reef surface and the spatial extent of wave breaking.

Similar spatial and temporal patterns of spectral wave energy occurred during the northeast monsoon experiment (Fig. 9g–f). Swell wave energy is prominent at most locations increasing from 20%–30% at windward locations to 50–60% at the leeward northwest shoreline and outer reef flat. Higher frequency energy (wind-wave energy and above) is dominant at windward locations at 35%–45% over the first three days of the measurement period (Fig. 9j–l). In contrast to the stronger westerly monsoon, this energy is still present at similar proportions on the leeward side of the island (Fig. 9g–i). This is attributed to the comparatively lower swell wave energy conditions, which amplifies the relative importance of higher frequency energy.

5.4. Spatial variation in total shoreline wave energy

While variations in *H*s and *H*max indicate small spatial differences around the island shoreline in each season, examination of the total variance associated with wave spectra highlights marked windward and leeward differences in total wave energy (Table 3). Results underscore the importance of tidal stage in providing an energy window for waves to access the shoreline and show that windward shorelines had more than twice the total wave energy at higher tidal stages. Such differences are attributed to the combination of swell and wind-wave activity on windward shorelines and the absence of wind activity at leeward shorelines. This finding has significant implications for the geomorphic activation of shorelines with an implied windward to leeward gradient and its reversal between monsoons.

5.5. Hulhudhoo reef structure and incident wave characteristics

Spatial and temporal variations in the magnitude and frequency of waves occurring on the Hulhudhoo reef flat and their transformation to the island shoreline reflect the interplay between the incident wave climate and reef platform structure (shape and topography). Observations that nearshore *H*s are not substantially different around the island shoreline are likely to reflect the near-complete refraction of swell around this relatively small and circular platform (Fig. 2) with minimal loss of energy prior to wave interaction with the reef surface. This implies that in this instance, platform size affords little protection in terms of incident wave energy to the leeward shoreline. The marked difference in nearshore wave conditions between seasons is a reflection of dramatic changes in incident wave climate between the higher westerly and lower northeast monsoon conditions as also identified by Kench et al. (2006).

However, small variations in *H*s values around the island were identified and marked differences in total wave energy were apparent with energy on windward shorelines being twice that on leeward beaches. Several factors can account for these observations. First, the combination of swell and wind wave energy increases total energy input to windward shorelines. Second, reef width has been identified in a number of studies as exerting a major control on the decay of energy in reformed waves as they propagate across reefs through turbulent and frictional dissipation of reef flat bores and reformed waves (Lowe et al., 2005; Kench and Brander, 2006a). Hulhudhoo is a circular sand cay island that occupies 49% of the reef surface and is positioned centrally on the platform. Reef width is narrow around the island perimeter (34–48 m) and is not likely to play a major role in producing the observed differences in shoreline wave energy.

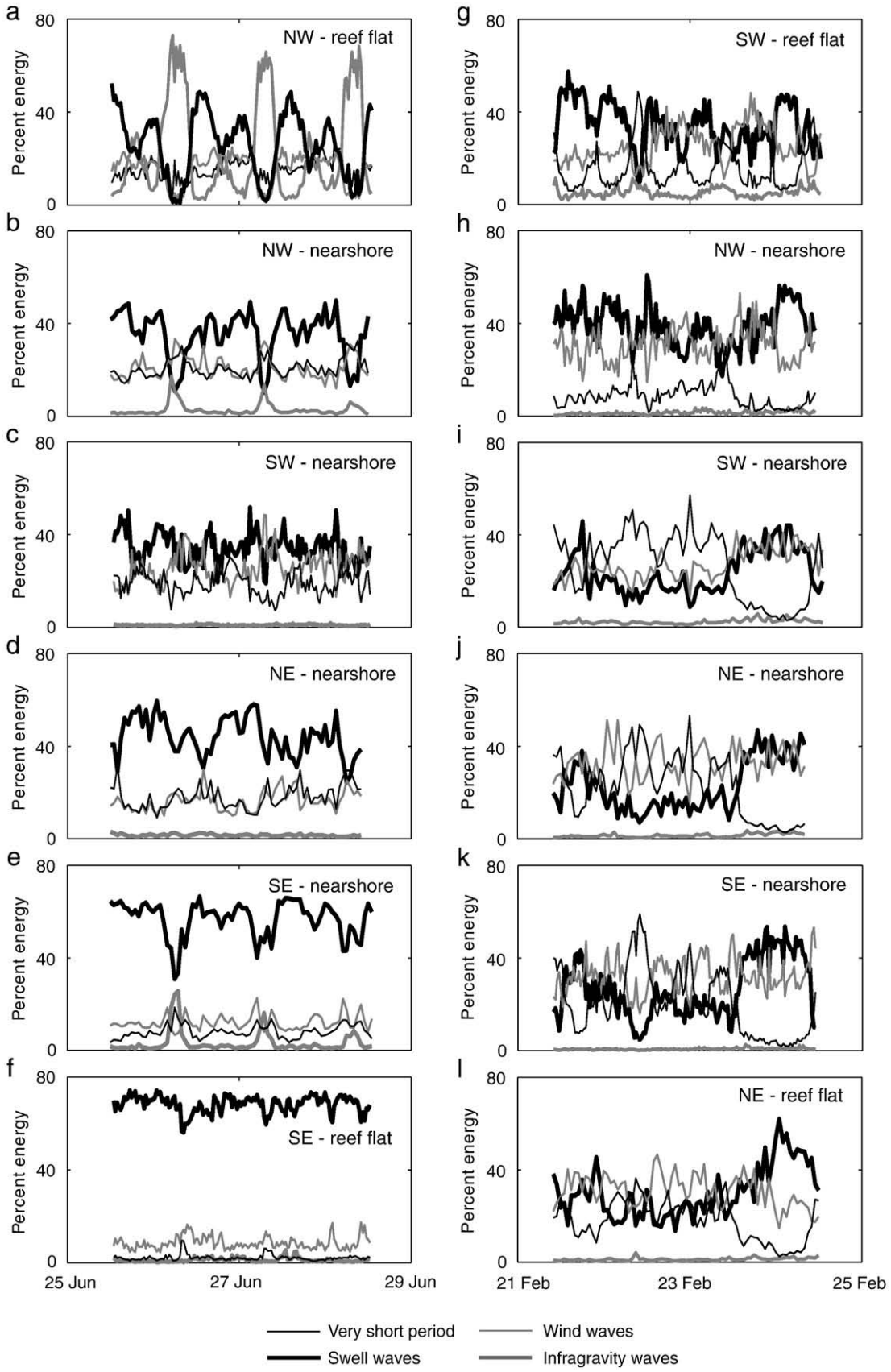

Fig. 9. Temporal and spatial comparison in the percentage of total wave energy divided into the different wave frequency bands at each instrument location through the experiment: a–f) westerly monsoon experiment (June); g–l) northeast monsoon (February). Location of instruments identified in each figure and shown in Fig. 2.

Third, reef elevation and changes in relative water depth also govern the height of waves on reef platforms. On Hulhudhoo, reef flat elevation varies by approximately 0.5 m. In particular, the north-eastern reef flat has a mean elevation 1.2 m below msl which is nearly 0.3 to 0.5 m lower in elevation than other sites (Table 1). Reef topography therefore helps account for the larger wave heights recorded at westerly and southeast shorelines during the westerly monsoon as waves are required to undergo greater shoaling across the higher elevation reef surfaces as opposed to the deeper northeast reef.

Reef elevation also controls the maximum potential wave height that can occur on the reef. A number of studies have identified depth limits that constrain maximum wave heights on reef flat surfaces (Nelson, 1994; Gourlay, 1994; Hardy and Young, 1996). Hardy and Young (1996) found that the upper boundary of significant and maximum wave heights is limited to less than 40% and 60% of the reef flat water depth respectively.

In terms of the potential for geomorphic work it is useful to examine measured versus potential wave conditions on the reef platform between seasons. In the westerly monsoon water depth versus *Hs* data from both outer reef locations plot as clusters of data that are well below the theoretical maximum wave height (Fig. 10a, b). This indicates that waves at these locations were not water depth constrained and are likely to represent incident swell propagating onto the outer reef without breaking. These waves are able to propagate directly onto the reef surface and subsequently shoal and break either across the reef flat or at the shoreline, accounting for the increase in wave height from reef edge to shoreline locations (Fig. 7).

The southeast, southwest and northwest shorelines exhibit marked linear trends suggesting wave heights are constrained by water depth (Fig. 10a, b). Of note, the southeast shoreline data plots on the established 0.4 *h* and 0.6 *h* relationships (Fig. 10a, b) and trends indicate that the shorelines are saturated with regard to wave energy under the westerly monsoon conditions. The northeastern nearshore location does not exhibit a linear trend, but data deviates to the right of both relationships with increasing water depth (Fig. 10a, b). This reflects the deeper reef on this side of the island with waves not constrained by water depth.

Under northeast monsoon conditions data from all instruments plot well under the limiting water depth constraint on wave height (Fig. 10c, d). This is expected given the lower incident wave heights (Fig. 4) and indicates the island shorelines are under-saturated with regard to wave energy under the northeast monsoon conditions.

5.6. Geomorphic implications

Observed spatial differences in wave energy on Hulhudhoo have left a distinct geomorphic imprint on coral reef structure, island morphology and shoreline morphodynamics. Differential exposure to wave energy has been used to account for a variety of geological and ecological processes in coral reef systems (Hopley, 1989). In particular energy gradients have been implicated as a control on differences in reef flat development and reef morphology (e.g. Roberts et al., 1977; Davies and Hopley, 1983; Roberts et al., 1992; Blanchon and Jones, 1995; Yamano et al., 2003).

Observations in this study indicate total wave energy input to the platform is greatest during the 8 month westerly monsoon period (Figs. 5, 6, 8; Table 3). Furthermore, during the westerly monsoon there is a distinct windward to leeward gradient in total wave energy input at the shoreline, which is most strongly expressed at high tide stages. Spatial differences in reef flat elevation reflect the imbalance of

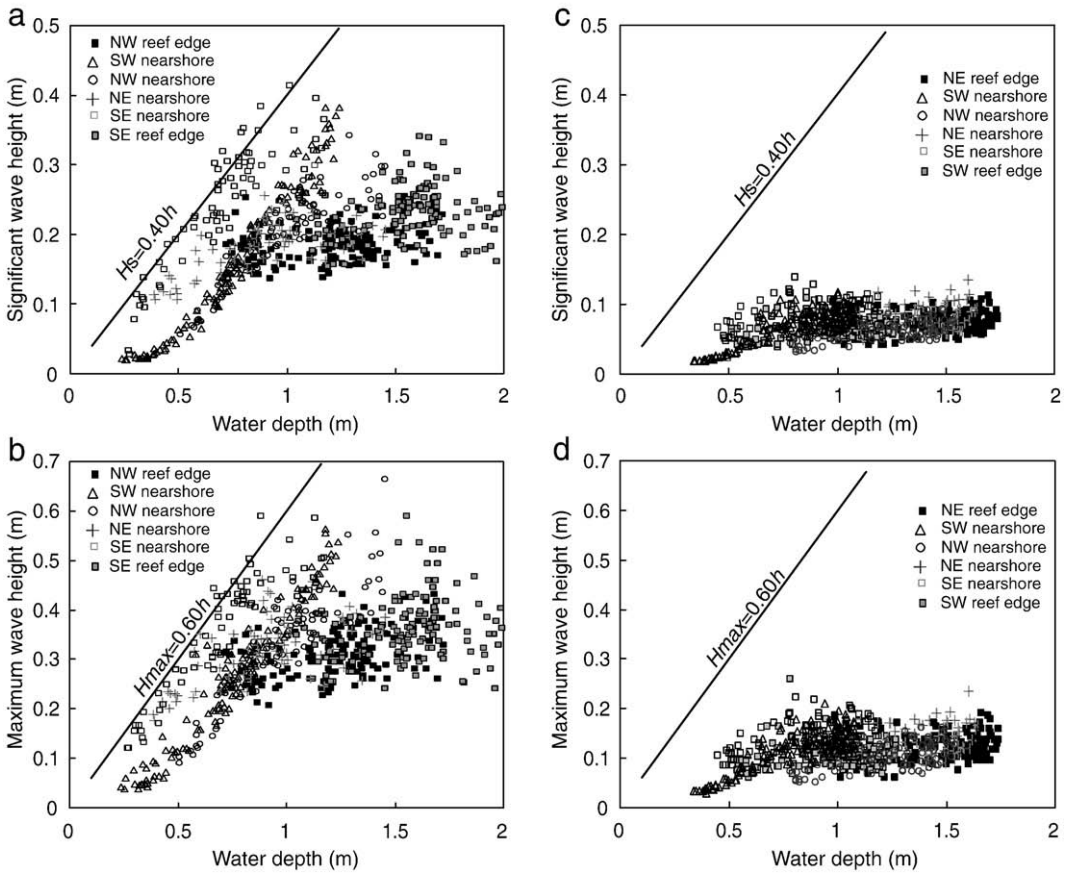

Fig. 10. Summary wave height versus water depth relationships for all instruments: a) Significant wave height versus water depth in westerly monsoon; b) Maximum wave height versus water depth in westerly monsoon; c) Significant wave height versus water depth in northeast monsoon; d) Maximum wave height versus water depth in northeast monsoon. Linear trends represent maximum wave heights for given water depth values after Hardy and Young (1996).

wave energy measured during this study. The mean reef flat elevation is approximately 0.2 m higher on the western side of the reef flat than eastern locations. Indeed the highest reef edge elevation is 1.04 m below msl, whereas the lowest reef edge elevation is 1.54 m below msl on the northeast reef rim (Table 1). The physical mechanisms driving this growth responses are likely to be a combination of greater wave energy, which is believed to promote more vigorous reef growth, and higher and sustained westerly wave setup providing increased accommodation space for vertical reef accretion.

Marked spatial differences in shoreline wave energy are also expressed in differences in island ridge elevation. Island surveys show that maximum island ridge elevations are substantially higher on the exposed western shoreline (2.5–1.92 m above msl) as opposed to the lower energy eastern exposure of the island (1.63–1.36 m above msl, Table 1). This marked morphological difference reflects higher total shoreline wave energy inputs along the western shoreline which is able to drive increased wave setup and runup processes, allowing shoreline sediment to be deposited at higher elevations along the western shoreline.

The monsoonal switch in wave energy gradient also drives seasonal morphodynamic adjustments of the reef island shoreline. Mid-to high tide wave energy at the island shoreline is sufficient to exceed the threshold conditions for medium-sized bioclastic sediment ($\sim$0.20 ms^{-1}, Kench and McLean, 1996). Visual observations also indicate that sediment transport is prevalent in the swash zone. Repeat surveys of the planform position of the island beach at different times across the monsoon seasons (Fig. 11) shows that Hulhudhoo beach shifts substantially between the northeast and western sides of the island where large lobes of beach material, up to 40 m in width, are temporarily located. This alongshore morphological adjustment of the beach reservoir amounts to approximately 46×10^3 m^3 per yr of alongshore sediment flux. The position of the sand lobes reflects the optimum location for sediment deposition around the island (nodal point) as a consequence of wave refraction around the reef structure and windward to leeward gradients in shoreline wave energy that are likely to promote alongshore currents. These observations suggest that the mobile island beach is sensitive to changes in wave approach. Differences in beach position around the island shoreline are likely to occur between seasons and between years (Fig. 11) as a consequence of interannual variations in monsoon intensity that controls both the magnitude and angle of incident waves.

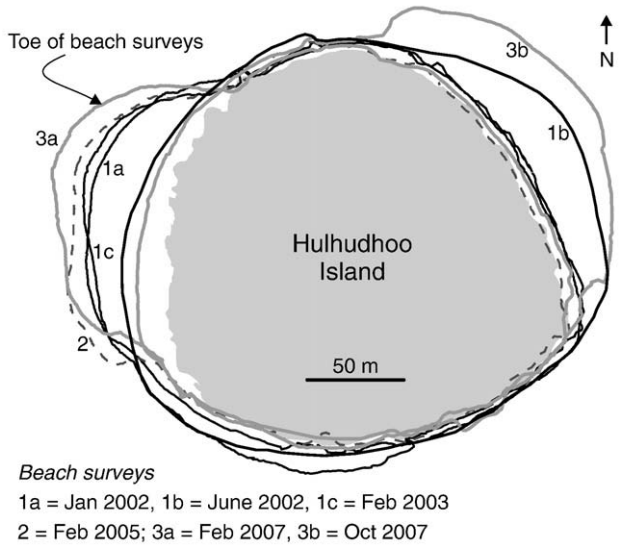

Fig. 11. Summary of Hulhudhoo Island seasonal and interannual beach changes. Lines represent the toe of beach surveyed using a Global Positioning System. Note surveys 1a–1c represent a full seasonal cycle in 2002–2003. 2 denotes the beach position following the Indian Ocean tsunami. 3a and 3b represent the end of the northeast westerly monsoon seasons respectively in 2007. Note the large changes in beach position which correspond to changes in monsoon wind and wave conditions.

6. Conclusions

Synchronous measurements of wave characteristics around the circular reef platform of Hulhudhoo Island identified distinct temporal and spatial patterns in the frequency and magnitude of waves impacting island shorelines. Results identified marked differences in the magnitude of wave energy on the reef platform between monsoon seasons with wave conditions during the westerly monsoon (Hmax 0.46–0.78 m) approximately an order of magnitude larger than the northeast monsoon. Each monsoon season was also characterised by a distinct spatial gradient in wave frequencies and energy. Results identified a distinct growth in wave height across the reef platform to island shoreline as a consequence of wave shoaling. Windward shorelines are characterized by waves in the wind and swell frequencies. However, wind wave energy was absent from leeward shorelines. As a consequence, compared to the leeward side of the island, windward shorelines typically experienced twice the total incident shoreline wave energy. Furthermore, the reversing monsoons ensure the windward to leeward energy gradient switches to opposite sides of the island between seasons.

Spatial and temporal patterns in wave processes modulate a number of geomorphic responses of the reef platform and island. First, the longer duration and larger incident wave energy experienced under the westerly monsoon is considered to have imparted distinct geomorphic imprints with higher reef growth ($+0.2$ m) and increased wave runup and consequently markedly higher island ridge elevations ($+0.7$ m) on the western reef flat and island shorelines respectively.

Second, incident gravity wave energy is able to propagate onto the reef platform and transform toward the island shoreline under mid- to high-tide stages. Consequently, there is a temporal window during each tidal cycle where waves of sufficient energy can stimulate sediment entrainment and transport at the island shoreline. Third, monsoonally driven changes in wave energy and windward to leeward gradients in wave energy drive large seasonal oscillations in the position of the mobile beach around the island shoreline. Such oscillations in beach position are also likely to be driven as a consequence of alongshore generated currents that are likely to be stimulated by the spatial differences in energy input to the island. Fourth, large energy differences between monsoons might be expected to exert an overriding control on island migration on the reef platform. However, monitoring observations suggest that the beach exhibits an equal morphological adjustment between monsoons. This suggests that differences in wave energetics between monsoons controls the pace at which morphological adjustment occurs, with adjustment occurring more rapidly in the westerly monsoon and occupying a larger period of the northeast monsoon season.

References

Abelson, A., Denny, M., 1997. Settlement of marine organisms in flow. Ann. Rev. Ecolog. Syst. 28, 317–339.
Blanchon, P., Jones, B., 1995. Marine-planation terraces on the shelf around Grand Cayman: a result of stepped Holocene sea-level rise. J. Coast. Res. 11, 1–33.
Brander, R.W., Kench, P.S., Hart, D.E., 2004. Spatial and temporal variations in wave characteristics across a reef platform, Warraber Island, Torres Strait, Australia. Mar. Geol. 207, 169–184.
Davies, P.J., Hopley, D., 1983. Growth fabrics and growth rates of Holocene reefs in the Great Barrier Reef. BMR J. Aust. Geol. Geophys. 8, 237–251.
Department of Meteorology, 1995. Some meteorological data 1966–1994. Report of the Meteorological Department, Government of Maldives.
Gerritsen, F., 1981. Wave attenuation and wave set-up on a coastal reef. Proceedings 17th International Conference on Coastal Engineering. ASCE, pp. 444–461.
Gourlay, M.R., 1988. Coral cays products of wave action and geological processes in a biogenic environment. Proceedings 6th International Coral Reef Symposium, Australia, pp. 491–496.

Gourlay, M.R., 1994. Wave transformation on a coral reef. Coast. Eng. 23, 17–42.
Gourlay, M.R., 1996. Wave set-up on coral reefs, 1, set-up and wave generated flow on an idealised two dimensional horizontal reef. Coast. Eng. 27, 161–1935.
Hamner, W.H., Wolanski, E., 1988. Hydrodynamic forcing functions and biological processes on coral reefs: a status review. Proceedings 6th International Coral Reef Symposium, vol. 1, pp. 8–12.
Hardy, T.A., Young, I.R., 1996. Field study of wave attenuation on an offshore coral reef. J. Geophys. Res. C101, 14311–14326.
Hardy, T.A., Young, I.R., Nelson, R.C., Gourlay, M.R., 1990. Wave attenuation on an offshore coral reef. Proceedings 22nd International Coastal Engineering Conference, vol. 1, pp. 330–344.
Hearn, C.J., 1999. Wave-breaking hydrodynamics within coral reef systems and the effect of changing relative sea level. J. Geophys. Res. 104 (C12), 30007–30019.
Hearn, C.J., Atkinson, M.J., Falter, J.L., 2001. A physical derivation of nutrient-uptake rates in coral reefs: effects of roughness and waves. Coral Reefs 20, 347–356.
Hopley, D., 1989. Coral reefs: zonation, zonality and gradients. Essen. Geogr. Arbeiten 18, 79–123.
Kench, P.S., McLean, R.F., 1996. Hydraulic characteristics of heterogeneous bioclastic deposits: new possibilities for interpreting environmental processes. Sedimentology 43, 531–540.
Kench, P.S., Brander, R.W., 2006a. Wave processes on coral reef flats: implications for reef geomorphology using Australian case studies. J. Coast. Res. 22, 209–223.
Kench, P.S., Brander, R.W., 2006b. Response of reef island shorelines to seasonal climate oscillations: South Maalhosmadulu atoll, Maldives. J. Geophys. Res. 111, F01001. doi:10.1029/2005JF000323.
Kench, P.S., McLean, R.F., Nichol, S.L., 2005. New model of reef-island evolution: Maldives, Indian Ocean. Geology 33, 145–148.
Kench, P.S., Brander, R.W., Parnell, K.E., McLean, R.F., 2006. Wave energy gradients across a Maldivian atoll: Implications for island geomorphology. Geomorphology 81, 1–17.
Lee, T.T., Black, K.P., 1978. The energy spectra of surf waves on a coral reef. Proceedings 16th International Conference on Coastal Engineering. ASCE, pp. 588–608.
Lowe, R.J., Falter, J.L., Bandet, M.D., Pawlak, G., Atkinson, M.J., Monismith, S.G., Koseff, J.R., 2005. Spectral wave dissipation over a barrier reef. J. Geophys. Res. 110, C04001. doi:10.1029/2004JC002711.
Lugo-Fernández, A., Hernández-Avila, M.L., Roberts, H.H., 1994. Wave energy distribution and hurricane effects on Margarita Reef, Southwestern Puerto Rico. Coral Reefs 13, 21–32.
Lugo-Fernández, A., Roberts, H.H., Wiseman Jr., W.J., 1998. Tide effects on wave attenuation and wave set-up on a Caribbean Coral Reef. Estuar. Coast. Shelf Sci. 47, 385–393.
Massel, S.R., 1996. On the largest wave height in water in water of constant depth. Ocean Eng. 23 (7), 553–573.
Massel, S.R., Brinkman, R.M., 1999. Measurement and modelling of wave propagation and breaking at steep reefs. In: Saxena, N. (Ed.), Recent Advances in Marine Science and Technology, 1998. Pacon Int.
Nakamori, T., Suzuki, A., Iryu, Y., 1992. Water circulation and carbon flux on Shiraho coral reef of the Rykuyu Island, Japan. Cont. Shelf Res. 12, 951–970.
Naseer, A., Hatcher, B.G., 2004. Inventory of the Maldives' coral reefs using morphometrics generated from Landsat ETM+ imagery. Coral Reefs 23, 161–168. doi:10.1007/s00338-003-0366-6.
Nelson, R.C., 1994. Depth limited design wave heights in very flat regions. Coast. Eng. 23, 43–59.
Nelson, R.C., 1997. Hydraulic roughness of coral reef platforms. Appl. Ocean Res. 18, 265–274.
Roberts, H.H., Suhayda, M., 1983. Wave current interactions on a shallow reef (Nicaragua). Coral Reefs 1, 209–260.
Roberts, H.H., Murray, S.P., Suhayda, J.N., 1977. Physical processes in a fore-reef shelf environment. Proceedings 3rd International Coral Reef Symposium. ASCE, Miami, pp. 507–515.
Roberts, H.H., Wilson, P.A., Lugo-Fernandez, A., 1992. Biologic and geologic responses to physical processes: examples from modern reef systems of the Caribbean–Atlantic region. Cont. Shelf Res. 12 (7/8), 809–834.
Samosorn, B., Woodroffe, C.D., 2008. Nearshore wave environments around a sandy cay on a platform reef, Torres Strait, Australia. Cont. Shelf Res. 28, 2257–2274.
Welch, P.D., 1967. The use of fast Fourier transform for the estimation of power spectra: a method based on time averaging over short, modified periodograms. IEEE Trans. Audio Electroacoust. 15, 70–73.
Yamano, H., Abe, O., Matsumoto, E., Kayanne, H., Yonekura, N., Blanchon, P., 2003. Influence of wave energy on Holocene coral reef development: an example from Ishigaki Island, Ryukyu Islands, Japan. Sediment. Geol. 159, 27–41.
Young, I.R., 1989. Wave transformation over coral reefs. J. Geophys. Res. 94, 9779–9789.
Young, I.R., 1999. Seasonal variability of the global ocean wind and wave climate. Int. J. Climatol. 19, 931–950.